Calculation Method Based on Analytical Formulas for Inrush Currents and Voltage Dips of Three-Phase Transformers: Energization from Delta-connected Side

Rikido Yonezawa [1,2], Shoji Kawasaki [2]
[1] Grid Innovation Research Laboratory, Central Research Institute of Electric Power Industry (CRIEPI), Kanagawa, Japan
[2] Graduate School of Science and Technology, Meiji University, Kanagawa, Japan
yonezawa@criepi.denken.or.jp, kawasaki@meiji.ac.jp

***Abstract*—A method has been developed to calculate the inrush currents and voltage dips during transformer energization with the same accuracy as electromagnetic transient (EMT) analysis. The developed method is based on analytical formulas obtained by directly solving the circuit equations formulated by simplifying the power system and transformer circuit. The calculation results of inrush currents and voltage dips under severe conditions are compared with EMT analysis results and confirmed to be in good agreement.**

***Index Terms*--Electromagnetic transient analysis, grid code, inrush currents, power quality, voltage dips**

I. Introduction

Excessive inrush currents can flow, leading to instantaneous voltage dips when energizing transformers at power stations and substations [1]. Owing to the potential for instantaneous voltage dips to disrupt consumer equipment, large magnitudes of such voltage dips necessitate appropriate preventive measures. In Japan, the Grid Interconnection Code mandates action when voltage dips exceeding 10% occur in the power distribution system [2]. Calculating voltage dips during transformer energization beforehand becomes imperative when inspecting substations or establishing connections for new customer equipment, allowing an assessment of the need for preventive measures.

It is recognized that electromagnetic transient (EMT) analysis programs such as EMTP [3], [4] and XTAP [5], [6] accurately estimate inrush currents and voltage dips [7]. Nonetheless, practical implementation is challenging owing to the fact that grid operator engineers, tasked with assessing countermeasure necessity, might not be well-versed in EMT analysis. This challenge becomes further pronounced with the increase in the number of renewable energy plants, as grid operators find themselves increasingly tasked with preliminary calculations to ascertain the need for countermeasures. This highlights the demand for a method that is both simple and highly accurate. Although a straightforward approach to calculating inrush currents and voltage dips has been introduced [8], it overlooks transient DC currents. Consequently, this approach yields higher inrush currents and voltage dips than EMT analysis. Although this rigorous assessment aligns with safety considerations when assessing transformers owned by power company, it could burden customers with undue, costly countermeasures based on conservative estimates. Hence, to ensure fairness, a simplified calculation method with maximal accuracy is imperative.

To address this concern, a method has been proposed in which inrush currents and voltage dips are computed using analytical formulas [9]. Notably, this method has potential practical application by enabling calculations of equal accuracy to EMT analysis. Achieving this level of accuracy merely entails inputting parameters specific to the transformer and power system. Note that, currently, analytical formulas have solely been derived for the scenario in which the transformer is energized from the star-connected side, rendering them inapplicable to cases involving delta-connected transformer energization.

In this paper, we derive analytical formulas for the current, flux and voltage when the transformer is energized from the delta-connected side, and we extend the method proposed by [9] to encompass delta-connected transformers. This proposed method is implemented as a tool that can be easily employed by engineers using the Python programming language. The accuracy of its calculations is verified by comparing the results with those obtained from an EMT analysis program. The findings demonstrate that this implemented tool offers sufficient accuracy for practical applications.

II. Circuit Definition

In the preliminary calculations of voltage dips during transformer energization, obtaining detailed information about transformers and power systems is not always feasible. As a result, the circuit to be analyzed must be constructible using readily available information.

Figure 1 shows the circuit from which the analytical formulas are derived in this paper. Compared with actual

Submitted to the 23rd Power Systems Computation Conference (PSCC 2024).

transformers and power systems, the following practical simplifications have been introduced:

- The power system is represented by a sinusoidal voltage source, $e = E_m \sin(\omega t + \theta)$, along with resistors and inductances connected in series. The transformer is modeled using Steinmetz's basic equivalent circuit [10]. The parameters for each phase are assumed to be three-phase balanced.
- The magnetizing circuit of the transformer is represented by a series connection of an ideal switch, Sw, and an inductance, L_{sat} (hereafter referred to as *saturation inductance*), at a completely saturated region [11]. The switch Sw is assumed to be open when the winding flux is below the saturation flux Φ_{sat} and closed when it exceeds Φ_{sat}.
- The circuit breakers CB_a, CB_b, and CB_c are considered ideal switches, with all three phases being turned on simultaneously.

These simplifications enable effective analysis within the given constraints of available information.

As indicated in the second point, the magnetizing circuit is significantly simplified by disregarding the magnetizing inductance during unsaturation and the hysteresis characteristic. This simplification not only permits the circuit to comprise solely linear elements but also reduces the number of unknown currents during unsaturation, thereby facilitating the derivation of analytical formulas. The primary goal of the preliminary voltage drip calculation is to determine the anticipated ratio under the most severe condition. Hence, the residual flux within the iron core is typically set to a substantial value, such as 0.8 per unit (p.u.) [7], and the voltage phase when the circuit breaker is turned on coincides with the moment when the flux is further elevated. Consequently, the impact of the period when the iron core remains unsaturated is relatively minimal; such a pronounced simplification does not yield significant errors in calculating the most rigorous circumstances.

The third point involves an assumption concerning circuit breaker operation. Although it is understood that circuit breaker conduction timing exhibits slight variations from phase to phase due to phenomena such as pre-arcing, these variations are negligible. Consequently, making this assumption does not pose an issue. However, it is important to note that in instances where circuit breakers operate independently in each phase, such as ultrahigh-voltage systems, the discrepancies in conduction timing across phases become substantial, subsequently affecting the magnitude of inrush currents. Therefore, it is important to acknowledge that the approach outlined in this paper is not applicable to such instances.

III. Derivation of Analytical Formulas

A. Circuit Equation Formulation

In the circuit illustrated in Fig. 1, the line currents in each primary phase are denoted by i_a, i_b, and i_c; the winding currents are i_{ab}, i_{bc}, and i_{ca}; the voltages across the magnetizing circuit are v_a, v_b, and v_c; the fluxes within the windings are Φ_a, Φ_b, and Φ_c; the voltages between phases are v_{ab}, v_{bc}, and v_{ca}; and the currents through the secondary delta winding are i_Δ, with a positive direction indicated by the arrows in Fig. 1. For simplicity, in this paper, we assume a turn ratio (voltage ratio) of 1:1 for the primary to secondary windings.

Although there are a total of seven unknown currents, Kirchhoff's current law effectively requires only four currents to deduce the remaining three. By deriving the circuit equations from Kirchhoff's voltage law and arranging them to focus on the four unknown currents i_a, i_b, i_{ab}, and i_Δ, we can derive the subsequent four equations.

$$e_a - e_b = R_b i_a + L_b \frac{di_a}{dt} + R_1 i_{ab} + L_1 \frac{di_{ab}}{dt} + v_a - R_b i_b - L_b \frac{di_b}{dt} \quad (1)$$

$$\begin{aligned} e_a - e_c &= (2R_b + R_1) i_a + (2L_b + L_1)\frac{di_a}{dt} \\ &\quad + R_b i_b + L_b \frac{di_b}{dt} - R_1 i_{ab} - L_1 \frac{di_{ab}}{dt} - v_c \end{aligned} \quad (2)$$

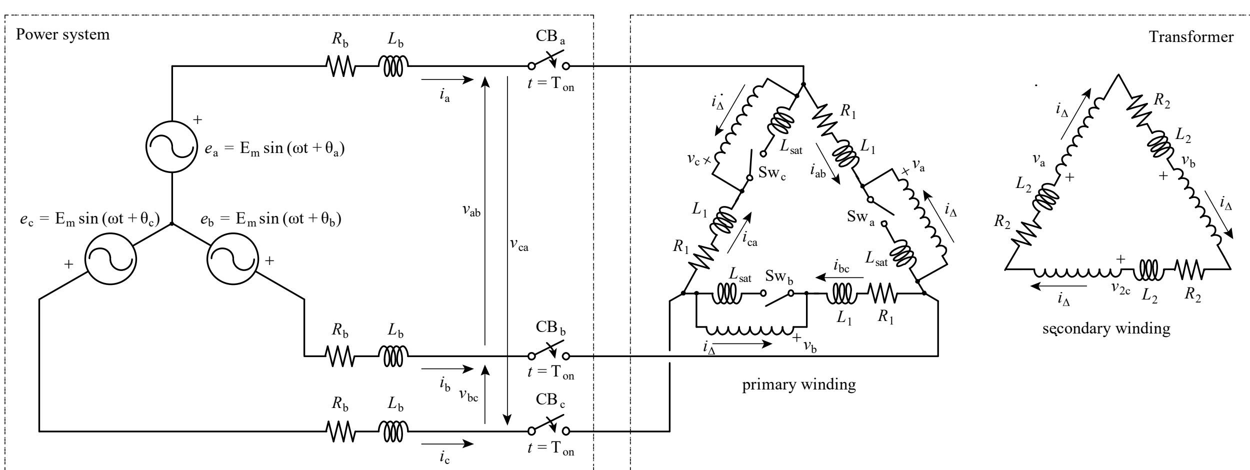

Figure 1. Circuit composed of a power system and a transformer as defined in this paper.

$$0=-R_1 i_a - L_1\frac{di_a}{dt}+R_1 i_b + L_1\frac{di_b}{dt}+3R_1 i_{ab}+3L_1\frac{di_{ab}}{dt} \\ +v_a+v_b+v_c \tag{3}$$

$$0=v_a+v_b+v_c+3R_2 i_\Delta+3L_2\frac{di_\Delta}{dt} \tag{4}$$

Equations (1) to (4) constitute the basic circuit equations.

In this circuit, the magnetizing circuit is represented by switches and saturation inductance, resulting in a total of eight modes, as shown in Table I. These modes correspond to various switch states within each phase, specifically the saturation status of each phase. Consequently, analytical formulas must be derived for each mode. In this paper, because of space limitation, we focus on elucidating the derivation of analytical formulas for mode 2ab. Analytical formulas for other modes can also be derived by the same procedure. For simplicity, we will assume that the mode is switched on at time 0 s.

TABLE I. OPEN/CLOSED STATE OF EACH SWITCH IN EACH MODE.

mode	Switch states of each phase		
	Sw_a	Sw_b	Sw_c
0	open	open	open
1a	close	open	open
1b	open	close	open
1c	open	open	close
2ab	close	close	open
2bc	open	close	close
2ca	close	open	close
3abc	close	close	close

B. Analytical Formulas for Mode 2ab

In mode 2ab, SW_a and SW_b are closed and SW_c is open in the circuit shown in Fig. 1. In this circuit, the following new conditions are added:

$$v_a = L_{sat}\frac{d(i_{ab}+i_\Delta)}{dt}, \\ v_b = L_{sat}\frac{d(i_{bc}+i_\Delta)}{dt}, \\ i_{ab}=i_a-i_\Delta. \tag{5}$$

Substituting the above equations into equations (1)–(4), and further eliminating v_c and arranging i_a, i_b, i_Δ in matrix form, we obtain

$$\begin{bmatrix} e_a-e_b \\ e_a-e_c \\ 0 \end{bmatrix} = p\begin{bmatrix} L_{11} & L_{12} & L_{13} \\ L_{21} & L_{22} & L_{23} \\ L_{31} & L_{32} & L_{33}\end{bmatrix}\begin{bmatrix} i_a \\ i_b \\ i_\Delta\end{bmatrix} + \begin{bmatrix} R_{11} & R_{12} & R_{13} \\ R_{21} & R_{22} & R_{23} \\ R_{31} & R_{32} & R_{33}\end{bmatrix}\begin{bmatrix} i_a \\ i_b \\ i_\Delta\end{bmatrix}, \tag{6}$$

where p is the differential operator and L_{mn} and R_{mn} are as follows:

$$L_{11}=L_b+L_d+L_1+L_{sat},\quad L_{12}=-L_d-L_b,\quad L_{13}=-L_1, \\ L_{21}=2(L_b+L_d+L_{sat}),\quad L_{22}=L_b+L_d+L_{sat}, \\ L_{23}=L_1+3L_2,\quad L_{31}=2L_1,\quad L_{32}=L_1,\quad L_{33}=-3(L_1+L_2), \\ R_{11}=R_1+R_b,\quad R_{12}=-R_b,\quad R_{13}=-R_1, \\ R_{21}=2R_b,\quad R_{22}=R_b,\quad R_{23}=R_1+3R_2, \\ R_{31}=2R_1,\quad R_{32}=R_1,\quad R_{33}=-3(R_1+R_2). \tag{7}$$

The Laplace transformation of the above equation yields

$$\left(\mathbf{k}\begin{bmatrix} E_a \\ E_b \\ E_c\end{bmatrix}+\begin{bmatrix}\phi_1 \\ \phi_2 \\ \phi_3\end{bmatrix}\right)=\mathbf{A}\begin{bmatrix} I_a \\ I_b \\ I_\Delta\end{bmatrix}, \tag{8}$$

where E_a, E_b, E_c, I_a, I_b, and I_Δ are the Laplace transforms of e_a, e_b, e_c, i_a, i_b, and i_Δ, respectively. In addition,

$$\phi_1 = L_{11}i_a(0)+L_{12}i_b(0)+L_{13}i_\Delta(0), \\ \phi_2 = L_{21}i_a(0)+L_{22}i_b(0)+L_{23}i_\Delta(0), \\ \phi_3 = L_{31}i_a(0)+L_{32}i_b(0)+L_{33}i_\Delta(0), \\ \mathbf{A}=\begin{bmatrix} A_{11} & A_{12} & A_{13} \\ A_{21} & A_{22} & A_{23} \\ A_{31} & A_{32} & A_{33}\end{bmatrix}, \\ A_{nm}=sL_{nm}+R_{nm}, \\ \mathbf{k}=\begin{bmatrix} k_{1a} & k_{1b} & k_{1c} \\ k_{2a} & k_{2b} & k_{2c} \\ k_{3a} & k_{3b} & k_{3c}\end{bmatrix}=\begin{bmatrix} 1 & -1 & 0 \\ 1 & 0 & -1 \\ 0 & 0 & 0\end{bmatrix}, \tag{9}$$

where $i_a(0)$, $i_b(0)$ and $i_\Delta(0)$ are the values of i_a, i_b, and i_Δ at time t of 0 s, and m and n are the arbitrary row and column numbers, respectively.

From the above equations, I_a, I_b, and I_Δ can be obtained by multiplying both sides of (8) by the inverse matrix of **A** from the left. Here, if the inverse of **A** is expressed using the cofactors $\tilde{A}_{11}$–$\tilde{A}_{33}$ of **A** and the determinant Δ, then I_a, I_b, and I_Δ are shown in the following equations:

$$\begin{bmatrix} I_a \\ I_b \\ I_\Delta\end{bmatrix}=\frac{1}{\Delta}\begin{bmatrix}\tilde{A}_{11} & \tilde{A}_{12} & \tilde{A}_{13} \\ \tilde{A}_{21} & \tilde{A}_{22} & \tilde{A}_{23} \\ \tilde{A}_{31} & \tilde{A}_{32} & \tilde{A}_{33}\end{bmatrix}\times\left(\mathbf{k}\begin{bmatrix} E_a \\ E_b \\ E_c\end{bmatrix}+\begin{bmatrix}\phi_1 \\ \phi_2 \\ \phi_3\end{bmatrix}\right). \tag{10}$$

If α, β, and γ are the solutions to the cubic equation with Δ being equal to 0, then the quotient of the cofactor and the determinant $\tilde{A}_{mn}$ / Δ can be decomposed as follows by partial fraction decomposition.

$$\frac{\tilde{A}_{mn}}{\Delta}=\frac{F_{2,mn}s+F_{1,mn}s+F_{0,mn}}{G_3(s-\alpha)(s-\beta)(s-\gamma)}=\frac{X_{mn}}{s-\alpha}+\frac{Y_{mn}}{s-\beta}+\frac{Z_{mn}}{s-\gamma}. \tag{11}$$

Here, $F_{2,mn}$ is the coefficient of s^2 in the cofactor $\tilde{A}_{mn}$, $F_{1,mn}$ is the coefficient of s^1 in $\tilde{A}_{mn}$, $F_{0,mn}$ is the coefficient of s^0 in $\tilde{A}_{mn}$, and G_3 is the coefficient of s^3 in the determinant Δ. X_{mn}, Y_{mn}, and Z_{mn} are respectively shown as

$$X_{mn} = \frac{F_{2,mn}\alpha^2 + F_{1,mn}\alpha + F_{0,mn}}{G_3(\alpha-\beta)(\alpha-\gamma)},$$
$$Y_{mn} = \frac{F_{2,mn}\beta^2 + F_{1,mn}\beta + F_{0,mn}}{G_3(\beta-\gamma)(\beta-\alpha)}, \quad (12)$$
$$Z_{mn} = \frac{F_{2,mn}\gamma^2 + F_{1,mn}\gamma + F_{0,mn}}{G_3(\gamma-\alpha)(\gamma-\beta)}.$$

For the coefficients G_3 of the determinant and the coefficients $F_{x,mn}$ of the cofactors, they can be derived by simple matrix operations, although they are rather long formulas that add up to several products of R_{mn} and L_{mn}. In this paper, α, β, and γ will be referred to as the *determinant solution* for convenience.

Substituting (11) into (10) and expanding the expression for I_a, we obtain

$$I_a = \begin{bmatrix} \frac{X_{11}}{s-\alpha} + \frac{Y_{11}}{s-\beta} + \frac{Z_{11}}{s-\gamma} \\ \frac{X_{12}}{s-\alpha} + \frac{Y_{12}}{s-\beta} + \frac{Z_{12}}{s-\gamma} \\ \frac{X_{13}}{s-\alpha} + \frac{Y_{13}}{s-\beta} + \frac{Z_{13}}{s-\gamma} \end{bmatrix}^T \times \left(\mathbf{k} \begin{bmatrix} E_a \\ E_b \\ E_c \end{bmatrix} + \begin{bmatrix} \phi_1 \\ \phi_2 \\ \phi_3 \end{bmatrix} \right). \quad (13)$$

Here, taking advantage of the fact that the product of $1/(s-\alpha)$ and E_a can be inverse Laplace transformed as shown in Appendix A, the inverse Laplace transform $L^{-1}[\cdot]$ of the above equation finally becomes

$$\begin{aligned} i_a &= L^{-1}[I_a] \\ &= \frac{\mathrm{E_m}}{\alpha^2+\omega^2}\left(K_{1\mathrm{Xa}}\cos\theta_a + K_{1\mathrm{Xb}}\cos\theta_b + K_{1\mathrm{Xc}}\cos\theta_c\right) \\ &\qquad \times\left(\omega e^{\alpha t} - \omega\cos\omega t - \alpha\sin\omega t\right) \\ &+ \frac{\mathrm{E_m}}{\alpha^2+\omega^2}\left(K_{1\mathrm{Xa}}\sin\theta_a + K_{1\mathrm{Xb}}\sin\theta_b + K_{1\mathrm{Xc}}\sin\theta_c\right) \\ &\qquad \times\left(\alpha e^{\alpha t} - \alpha\cos\omega t + \omega\sin\omega t\right) \\ &+ \frac{\mathrm{E_m}}{\beta^2+\omega^2}\left(K_{1\mathrm{Ya}}\cos\theta_a + K_{1\mathrm{Yb}}\cos\theta_b + K_{1\mathrm{Yc}}\cos\theta_c\right) \\ &\qquad \times\left(\omega e^{\beta t} - \omega\cos\omega t - \beta\sin\omega t\right) \\ &+ \frac{\mathrm{E_m}}{\beta^2+\omega^2}\left(K_{1\mathrm{Ya}}\sin\theta_a + K_{1\mathrm{Yb}}\sin\theta_b + K_{1\mathrm{Yc}}\sin\theta_c\right) \\ &\qquad \times\left(\beta e^{\beta t} - \beta\cos\omega t + \omega\sin\omega t\right) \\ &+ \frac{\mathrm{E_m}}{\gamma^2+\omega^2}\left(K_{1\mathrm{Za}}\cos\theta_a + K_{1\mathrm{Zb}}\cos\theta_b + K_{1\mathrm{Zc}}\cos\theta_c\right) \\ &\qquad \times\left(\omega e^{\gamma t} - \omega\cos\omega t - \gamma\sin\omega t\right) \\ &+ \frac{\mathrm{E_m}}{\gamma^2+\omega^2}\left(K_{1\mathrm{Za}}\sin\theta_a + K_{1\mathrm{Zb}}\sin\theta_b + K_{1\mathrm{Zc}}\sin\theta_c\right) \\ &\qquad \times\left(\gamma e^{\gamma t} - \gamma\cos\omega t + \omega\sin\omega t\right) \\ &+ K_{1\mathrm{X}\phi}e^{\alpha t} + K_{1\mathrm{Y}\phi}e^{\beta t} + K_{1\mathrm{Z}\phi}e^{\gamma t}, \end{aligned} \quad (14)$$

where

$$\mathbf{K}_m = \begin{bmatrix} K_{m\mathrm{Xa}} & K_{m\mathrm{Ya}} & K_{m\mathrm{Za}} \\ K_{m\mathrm{Xb}} & K_{m\mathrm{Yb}} & K_{m\mathrm{Zb}} \\ K_{m\mathrm{Xc}} & K_{m\mathrm{Yc}} & K_{m\mathrm{Zc}} \\ K_{m\mathrm{X}\phi} & K_{m\mathrm{Y}\phi} & K_{m\mathrm{Z}\phi} \end{bmatrix} = \begin{bmatrix} k_{1\mathrm{a}} & k_{2\mathrm{a}} & k_{3\mathrm{a}} \\ k_{1\mathrm{b}} & k_{2\mathrm{b}} & k_{3\mathrm{b}} \\ k_{1\mathrm{c}} & k_{2\mathrm{c}} & k_{3\mathrm{c}} \\ \phi_1 & \phi_2 & \phi_3 \end{bmatrix} \begin{bmatrix} X_{m1} & Y_{m1} & Z_{m1} \\ X_{m2} & Y_{m2} & Z_{m2} \\ X_{m3} & Y_{m3} & Z_{m3} \end{bmatrix}, \quad (15)$$

and m is the row number. $\mathbf{K}_m$ is an important parameter for obtaining the currents in each phase as well as the determinant solution, and these will be referred to as *K values* in this paper. As is clear from (14), i_a is expressed as the sum of exponential and trigonometric functions. Here, the exponential functions correspond to the transient DC component present in the inrush currents, arising from the abrupt change in circuit conditions due to magnetic saturation. For i_b and i_Δ, the K values shown in (15) (m = 2 for i_b and m = 3 for i_Δ) can be calculated similarly by substituting them into (14).

Next, the winding flux of each phase is derived. The flux of a saturated phase can be obtained by adding the product of the saturation inductance and current to the saturation flux Φ_{sat}. Thus, the fluxes Φ_a and Φ_b are calculated as

$$\Phi_a = \Phi_{sat} + L_{sat}(i_{ab} + i_\Delta), \quad (16)$$

$$\Phi_b = \Phi_{sat} + L_{sat}(i_b + i_{ab} + i_\Delta) \quad \because i_{bc} = i_b + i_{ab}. \quad (17)$$

The flux Φ_c, of the phase c winding, which is unsaturated, is calculated by integrating the winding voltage. Substituting (5) into (3) and rearranging for v_c, we obtain the following equation:

$$v_c = -2L_{sat}\frac{\mathrm{d}i_a}{\mathrm{d}t} - L_{sat}\frac{\mathrm{d}i_b}{\mathrm{d}t} - 3R_2 i_\Delta - 3L_2\frac{\mathrm{d}i_\Delta}{\mathrm{d}t}. \quad (18)$$

Therefore, Φ_c is given by

$$\begin{aligned} \Phi_c &= \int v_c dt \\ &= -2L_{sat}i_a - L_{sat}i_b - 3R_2 q_\Delta - 3L_2 i_\Delta + C, \end{aligned} \quad (19)$$

where C is the integration constant and q_Δ is

$$q_\Delta = \int i_\Delta dt. \quad (20)$$

Since Φ_c (0), i_a (0), i_b (0), and i_Δ (0) are known, C in the above equation can be obtained by substituting them into the above equation. Moreover, q_Δ can be easily calculated since it is the integral of i_Δ expressed as a combination of trigonometric and exponential functions. For this reason, the derivation is omitted because of space limitation.

Finally, the line voltages v_{ab}, v_{bc}, and v_{ca} are derived. From Kirchhoff's voltage law, each can be calculated as:

$$\begin{aligned} v_{ab} &= R_b i_b + L_b \frac{di_b}{dt} - e_b + e_a - R_b i_a - L_b \frac{di_a}{dt}, \\ v_{bc} &= -R_b i_a - L_b \frac{di_a}{dt} - e_c + e_b - 2R_b i_b - 2L_b \frac{di_b}{dt}, \\ v_{ca} &= 2R_b i_a + 2L_b \frac{di_a}{dt} - e_a + e_c + R_b i_b + L_b \frac{di_b}{dt}. \end{aligned} \tag{21}$$

In the above equations, i_a and i_b are composed of exponential and trigonometric functions, whose derivatives can also be easily derived, so the analytical expressions for each are omitted because of space limitation.

The above are the analytical formulas for current, flux, and voltage for mode 2ab. When two phases other than phases a and b are saturated, the circuit configuration remains unaltered; only the phase of the power supply varies. Consequently, the analytical formulas for current, flux, and voltage can be derived utilizing the same approach as elucidated in the previous sections. Modes 1a, 1b, 1c, and 3abc follow a similar pattern. By substituting the conditions deduced from the open/closed state of the switch for each mode into (1) to (4), and subsequently performing calculations on the resultant matrices (2x2 for mode 1 and 4x4 for mode 3) using analogous procedures, each current is ultimately computed following the pattern of (14), albeit with varying numbers of terms. The derivation of flux and voltage follows a parallel methodology. Additionally, Appendix B presents the analytical formulas for the currents for Modes 0 and 1a.

As is clear from the analytical formulas obtained, they can be calculated using trigonometric and exponential functions and basic arithmetic operations, so they can be easily calculated using spreadsheet software such as Excel as well as numerical calculation platforms such as MATLAB and Python.

It should be noted that the analytical formulas derived in this paper targets transformers with a delta–delta connection as shown in Fig. 1. However, a similar procedure can be followed to create circuit equations and derive analytical formulas for transformers with a delta–star connection. The derivation of the analytical formulas for the delta–star connection will be reserved for a subsequent paper.

IV. Calculation Method for Inrush Currents and Voltage Dips Using Analytical Formulas

By employing the analytical formulas for each mode, we can determine inrush currents and voltage dips following the process outlined in Fig. 2.

In Step 1, initial values essential for analysis are defined, including power system and transformer parameters outlined in Table II, the timing of circuit breaker activation (or initial power source phase), residual flux in each phase (Φ_{Ra}, Φ_{Rb}, and Φ_{Rc}), calculation time step (Δt), and maximum calculation time (T_{max}). These values are simultaneously employed to calculate determinant solutions and K values for each mode. The initial current values for each phase are set to zero. The initial flux values for each phase are set to Φ_{Ra}, Φ_{Rb}, and Φ_{Rc}. Mode 0 is designated as the starting mode.

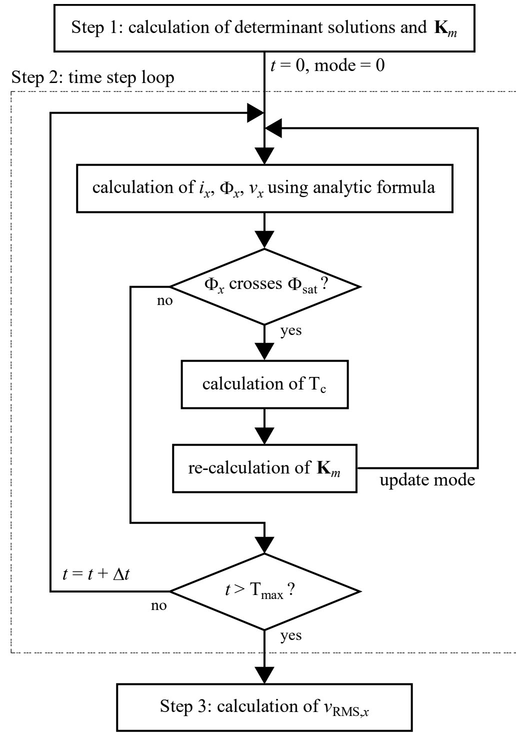

Figure 2. Calculation procedure of the proposed method.

In Step 2, the values established in Step 1 are substituted into the analytical formulas of the current mode. This enables the calculation of current, flux, and voltage for each calculation time step. Additionally, at each Δt interval, an assessment is conducted to ascertain whether the absolute flux value surpasses or dips below the saturation flux Φ_{sat}. If such an event occurs, the corresponding time instant T_c is determined. Several methods, including the Newton–Raphson approach, can be employed to calculate T_c. Alternatively, since flux changes occur gradually, even a simple approximation function (e.g., linear approximation) can sufficiently predict T_c from past flux values. After determining T_c, the subsequent mode is identified for transition, with the current and flux values at T_c being set as initial values for the next mode.

This procedure is iterated until t reaches T_{max}, triggering Step 3. In this step, the root mean square (RMS) voltage waveforms $v_{RMS,ab}$, $v_{RMS,bc}$, and $v_{RMS,ca}$ are respectively computed from the voltages v_{ab}, v_{bc}, and v_{ca} obtained thus far, using the formula

$$v_{RMS} = \sqrt{(1/T_s)\int_t^{t+T_s} v^2 dt}\ , \tag{22}$$

where T_s represents the period of system frequency.

Upon obtaining the RMS value of the voltage, it becomes straightforward to calculate both its minimum value and the voltage drip (which indicates the extent of decline from the base voltage).

As outlined, simple arithmetic operations encompassing analytical formula computation and mode transitioning based on flux variations are sufficient for calculating inrush currents and voltage dips. The following section will delve into the verification of this prototype program.

V. Verification

The method proposed in the previous section is validated using the transformer and power system outlined in Table II. The calculated results of the inrush currents and voltage dips are compared with the outcomes of EMT analysis. The current-flux characteristics of the magnetizing circuit are assumed as described in Fig. 3.

Calculation is performed using a prototype Python program for the proposed method. The calculation employs a time step of 10 µs and runs for 200 ms. The leakage inductance is divided in half for the primary and secondary windings. The saturation flux is 33.64 Wb, which is the intersection of the vertical axis (zero current) and the straight line L in the section around 15 A where the slope is smallest among the characteristics shown in Fig. 3. The saturation inductance is obtained as 44.77 mH, which is the slope of the same segment. The voltage phase when the circuit breaker is turned on is 330 degrees, and the residual fluxes are $\Phi_{Ra} = 0.693$, $\Phi_{Rb} = -0.693$, and $\Phi_{Rc} = 0$ (units are all in p.u.).

For EMT analysis, XTAP [5], [6], a standard EMT analysis program utilized in Japan, is employed. The magnetizing circuit model incorporates hysteresis and takes the characteristics outlined in Fig. 3. Other circuit parameters, calculation time step, and calculation time are the same as those for the proposed method.

Figure 4 illustrates the waveforms of currents i_a, i_b, and i_c, and the RMS voltages $v_{RMS,ab}$, $v_{RMS,bc}$, and $v_{RMS,ca}$, as calculated by both the proposed method and EMT analysis. The solid line represents the proposed method (Proposed), whereas the dashed line depicts the results of EMT analysis (EMT). As depicted, the agreement between the two results is consistent across not only the initial waveform but also the 10th cycle waveform. Table III shows the peak values of i_b from the first to the tenth cycle. This confirms the comparable accuracy of the proposed method to EMT analysis. Although not shown here owing to

TABLE II. Calculation procedure of the proposed method.

	unit	test case
(Parameters of the transformer)		
Rated power S	kVA	750
Rated voltage V_1/V_2	kV	6.6/0.21
Winding resistance R_1/R_2	Ω	0.188/0.19m
Leakage inductance L_{12}	%	3.83
(Parameters of the power system)		
System voltage E	kV	6.6
System frequency f	Hz	50
System impedance R_b / X_b	Ω	0.5/1.57

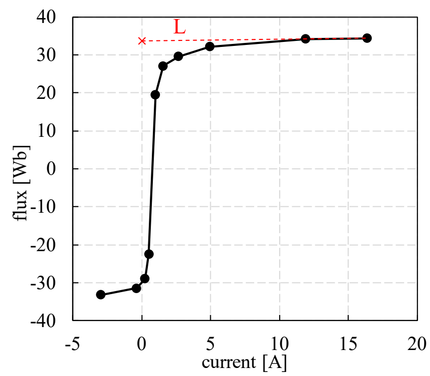

Figure3. Current-flux characteristics of the test case. The line L is an extrapolation of the slope in the section around 15 A.

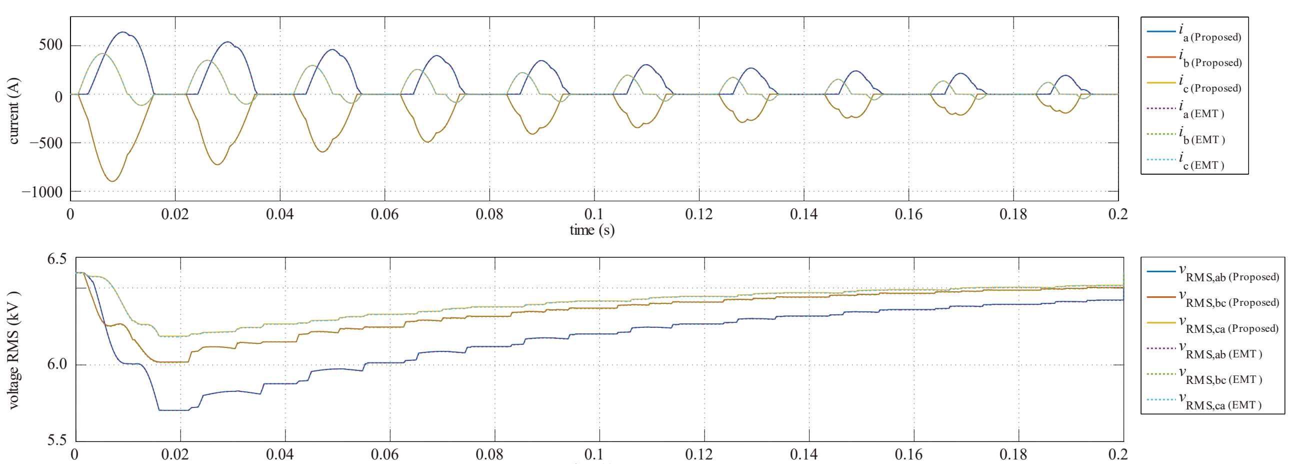

Figure 4. Inrush current and RMS voltage waveforms calculated by the proposed method and EMT analysis. The waveforms from the proposed method and the EMT analysis are almost overlapping.

TABLE III. COMPARISON OF CURRENT PEAK VALUES PER CYCLE.

cycle	EMT [A]	Proposed method [A]
1	−898.91	−899.21
2	−726.00	−726.47
3	−594.79	−595.40
4	−492.41	−493.13
5	−410.78	−411.60
6	−344.52	−345.44
7	−289.95	−290.96
8	−244.44	−245.55
9	−214.68	−215.26
10	−193.47	−194.16

space limitation, the flux and voltage waveforms similarly exhibit alignment.

Since the magnetizing circuit was simplified in the proposed method, errors due to this simplification were a concern, but they are not confirmed in the ranges shown in Fig. 4. Figure 5 shows the expanded waveforms for i_a, i_b, and i_c for the periods before and after the mode 0 transition. Owing to the smooth current–flux characteristic in EMT analysis, the current waveform maintains a smooth profile in the unsaturated magnetizing inductance region, in contrast to the proposed method. However, the current magnitude within this segment is notably smaller than that at saturation. Consequently, the changes in flux and voltage stemming from this difference remain minimal. This observation is particularly prominent in the analysis under severe conditions characterized by deep saturation. Hence, when considering the overall calculation, the impact of the unsaturation period on the inrush current and RMS voltage is deemed insignificant.

VI. CONCLUSION

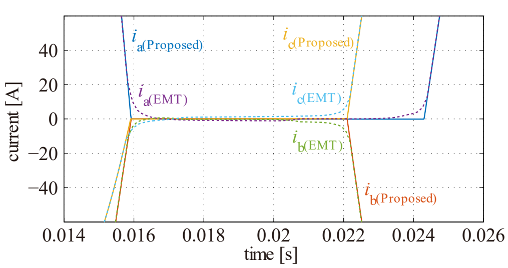

Figure 5. Expanded inrush current waveforms calculated by the proposed method and EMT analysis for the periods before and after the mode 0 transition

In this paper, a simple calculation method is studied to accurately calculate the inrush currents and voltage dips obtained when the delta-connected side of a transformer is energized without using EMT analysis. We devised a method to represent the magnetizing circuit of a transformer and derived analytical formulas for the voltage and current in each part of the system, taking into account the transient DC component. Furthermore, we proposed a simplified calculation method to ascertain the inrush currents and voltage dips utilizing these analytical formulas. As a result of verification, it was confirmed that the proposed method has approximately the same accuracy as EMT analysis.

Using the proposed method, even engineers not proficient in EMT analysis can easily and accurately calculate the inrush currents and voltage dips. Unlike conventional simplified methods, this is a high-accuracy calculation considering the transient DC current, thereby reducing the risk of erroneously deeming unnecessary measures as required. Additionally, since the proposed method is based on analytical formulas, it can be implemented in various platforms without restrictions, including software like MATLAB, Python, or Excel programs.

Looking ahead, we envisage the development of this methodology into a user-friendly web application, facilitating easy utilization by engineers in need of such calculations.

REFERENCES

[1] L. F. Blume, A. Boyajian, G. Camilli, T. C. Lennox, S. Minneci and V. M. Montsinger, Transformer Engineering, *A treatise on the theory, operation, and application of transformers*, New York: Wiley, 1951.

[2] The Japan Electric Association, *Grid-interconnection Code*, JEAC 9701-2019, 2019. (in Japanese)

[3] H. W. Dommel, *Electromagnetic transients program reference manual (EMTP theory book)*, Portland, OR, U.S.A., BPA, 1986.

[4] EMTP website [Online]. Available: https://emtp.com.

[5] T. Noda, K. Takenaka and T. Inoue, "Numerical integration by the 2-stage diagonally implicit Runge–Kutta method for electromagnetic transient simulations," *IEEE Trans. Power Delivery*, vol. 24, no. 1, pp.390-399, 2009.

[6] XTAP website [Online]. Available: https://www.xtap.org.

[7] CIGRE Working Group C4.307, *Transformer energization in power systems: a study guide*, CIGRE brochure, vol. 568, 2014.

[8] Y. Nakachi, T. Fukae, T. Sugahara, H. Nakamura, M. Koyama and F. Ueda, "Development of a simplified calculation tool for voltage drop caused by transformer inrush in distribution system," *IEEJ Trans. Power and Energy*, vol. 132, no. 2, pp. 197-206, 2012. (in Japanese)

[9] R. Yonezawa, "A simplified calculation method based on analytical formulas for inrush currents and voltage drop rates during energization from the star connected side", CRIEPI report GD22008, 2023. (in Japanese)

[10] C. P. Steinmetz, *Theory and calculation of alternating current phenomena third edition*, McGraw publishing, New York, 1900.

[11] J. E. Holcomb, "Distribution transformer magnetizing inrush current," *Trans of the AIEE. Part III: Power apparatus and systems*, vol. 80, issue 3, pp. 697-702, April, 1961.

APPENDIX

A. *Derivation procedure of inverse Laplace transform*

Since E_a is the Laplace transform of $E_m \sin(\omega t + \theta_a)$, the product of $1 / (s - \alpha)$ and E_a is

$$\frac{1}{s-\alpha}E_{\rm a}=\frac{{\rm E_m}}{s-\alpha}\left(\frac{\omega}{s^2+\omega^2}\cos\theta_a+\frac{s}{s^2+\omega^2}\sin\theta_a\right)$$
$$={\rm E_m}\cos\theta_a\frac{1}{s-\alpha}\frac{\omega}{s^2+\omega^2}+{\rm E_m}\sin\theta_a\frac{1}{s-\alpha}\frac{s}{s^2+\omega^2}, \tag{23}$$

where

$$\frac{1}{s-\alpha}\frac{\omega}{s^2+\omega^2}=\frac{{\rm P}}{s-\alpha}+\frac{{\rm Q}s}{s^2+\omega^2}+\frac{{\rm R}}{s^2+\omega^2},$$
$${\rm P}=\frac{\omega}{\alpha^2+\omega^2},\quad {\rm Q}=\frac{-\omega}{\alpha^2+\omega^2},\quad {\rm R}=\frac{-\alpha\omega}{\alpha^2+\omega^2} \tag{24}$$

$$\frac{1}{s-\alpha}\frac{s}{s^2+\omega^2}=\frac{{\rm M}}{s-\alpha}+\frac{{\rm N}s}{s^2+\omega^2}+\frac{{\rm O}}{s^2+\omega^2},$$
$${\rm M}=\frac{\alpha}{\alpha^2+\omega^2},\quad {\rm N}=\frac{-\alpha}{\alpha^2+\omega^2},\quad {\rm O}=\frac{\omega^2}{\alpha^2+\omega^2}. \tag{25}$$

Therefore, the inverse Laplace transform of (23) becomes

$$L^{-1}\left[\frac{1}{s-\alpha}E_{\rm a}\right]$$
$$=\frac{{\rm E_m}\cos\theta_a}{\alpha^2+\omega^2}\left(\omega e^{\alpha t}-\omega\cos\omega t-\alpha\sin\omega t\right)$$
$$+\frac{{\rm E_m}\sin\theta_a}{\alpha^2+\omega^2}\left(\alpha e^{\alpha t}-\alpha\cos\omega t+\omega\sin\omega t\right). \tag{26}$$

B. Analytical formulas for currents in Modes 0 and 1a

In mode 0, since all phases are unsaturated, SW_a, SW_b and SW_c are all open. In this circuit, the following new conditions are added:

$$i_\Delta=-i_{\rm ab}=-i_{\rm bc}=-i_{\rm ca} \tag{27}$$

$$i_{\rm a}=i_{\rm b}=i_{\rm c}=0 \tag{28}$$

By substituting the above equations into (1)–(4) and rearranging, the following formula for i_Δ is derived.

$$i_\Delta=i_\Delta(0)e^{-\frac{R_1+R_2}{L_1+L_2}t} \tag{29}$$

where $i_\Delta(0)$ is the value of i_Δ at time t of 0 s.

In Mode 1a, within the circuit shown in Fig. 1, SW_a is closed, while SW_b and SW_c remain open. In this circuit, the following new conditions are added:

$$v_{\rm a}=L_{\rm sat}\frac{{\rm d}(i_{\rm ab}+i_\Delta)}{{\rm d}t} \tag{30}$$

$$i_\Delta=-i_{\rm bc}=-i_{\rm ca} \tag{31}$$

$$i_{\rm ab}=i_{\rm a}-i_\Delta \tag{32}$$

By substituting the above equations into (1)–(4) and further eliminating $v_{\rm b}$ and $v_{\rm c}$, the matrix form for $i_{\rm a}$ and i_Δ is obtained as follows.

$$\begin{bmatrix} e_{\rm a}-e_{\rm b} \\ 0 \end{bmatrix}=p\begin{bmatrix} L_{11} & L_{12} \\ L_{21} & L_{22} \end{bmatrix}\begin{bmatrix} i_{\rm a} \\ i_\Delta \end{bmatrix}+\begin{bmatrix} R_{11} & R_{12} \\ R_{21} & R_{22} \end{bmatrix}\begin{bmatrix} i_{\rm a} \\ i_\Delta \end{bmatrix} \tag{33}$$

where L_{mn} and R_{mn} are as follows:

$$\begin{aligned} &L_{11}=L_{\rm b}+L_1+L_{\rm sat}+L_{\rm b},\quad L_{12}=-L_1, \\ &L_{21}=L_1,\quad L_{22}=-3(L_1+L_2), \\ &R_{11}=R_{\rm b}+R_1+R_{\rm b},\quad R_{12}=-R_1, \\ &R_{21}=R_1,\quad R_{22}=-3(R_1+R_2). \end{aligned} \tag{34}$$

By applying the Laplace transform to the above equations and rearranging it in the same manner as for Mode 2ab, as described in Section III.B, the final analytical formula for $i_{\rm a}$ is obtained as follows.

$$\begin{aligned} i_{\rm a}&=L^{-1}\left[I_{\rm a}\right] \\ &=\frac{{\rm E_m}}{\alpha^2+\omega^2}\left(K_{\rm 1Xa}\cos\theta_{\rm a}+K_{\rm 1Xb}\cos\theta_{\rm b}+K_{\rm 1Xc}\cos\theta_{\rm c}\right) \\ &\qquad\times\left(\omega e^{\alpha t}-\omega\cos\omega t-\alpha\sin\omega t\right) \\ &+\frac{{\rm E_m}}{\alpha^2+\omega^2}\left(K_{\rm 1Xa}\sin\theta_a+K_{\rm 1Xb}\sin\theta_{\rm b}+K_{\rm 1Xc}\sin\theta_{\rm c}\right) \\ &\qquad\times\left(\alpha e^{\alpha t}-\alpha\cos\omega t+\omega\sin\omega t\right) \\ &+\frac{{\rm E_m}}{\beta^2+\omega^2}\left(K_{\rm 1Ya}\cos\theta_{\rm a}+K_{\rm 1Yb}\cos\theta_{\rm b}+K_{\rm 1Yc}\cos\theta_{\rm c}\right) \\ &\qquad\times\left(\omega e^{\beta t}-\omega\cos\omega t-\beta\sin\omega t\right) \\ &+\frac{{\rm E_m}}{\beta^2+\omega^2}\left(K_{\rm 1Ya}\sin\theta_{\rm a}+K_{\rm 1Yb}\sin\theta_{\rm b}+K_{\rm 1Yc}\sin\theta_{\rm c}\right) \\ &\qquad\times\left(\beta e^{\beta t}-\beta\cos\omega t+\omega\sin\omega t\right) \\ &+K_{1{\rm X}\phi}e^{\alpha t}+K_{1{\rm Y}\phi}e^{\beta t}, \end{aligned} \tag{35}$$

where α and β are the determinant solution, and $K_{\rm 1Xa}$, $K_{\rm 1Xb}$, $K_{\rm 1Xc}$, $K_{\rm 1Ya}$, $K_{\rm 1Yb}$, $K_{\rm 1Yc}$, $K_{1{\rm X}\phi}$ and $K_{1{\rm Y}\phi}$ are K values, respectively.